Title
Dynamic Modeling of a Solid Oxide Fuel Cell Combined Heat and Power System With Thermal Storage for Commercial Building Applications

ISBN
978-0-7918-4881-4

Authors
Nanaeda, Kimihiro
Mueller, Fabian
Brouwer, Jacob
et al.

Publication Date
2009

DOI
10.1115/fuelcell2009-85169

Proceedings of ASME 2009 Seventh International Fuel Cell Science, Engineering and Technology Conference
FuelCell2009
June 8-10, 2009 Newport Beach, California, USA

FuelCell2009-85169

DYNAMIC MODELING OF A SOLID OXIDE FUEL CELL COMBINED HEAT AND POWER SYSTEM WITH THERMAL STORAGE FOR COMMERCIAL BUILDING APPLICATIONS

Kimihiro Nanaeda, Fabian Mueller, Jacob Brouwer, Scott Samuelsen
Mechanical and Aerospace Engineering Department
National Fuel Cell Research Center, University of California, Irvine, CA

ABSTRACT

A dynamic model of an integrated solid oxide fuel cell (SOFC) combined heat and power (CHP) system has been developed. The model was developed by modifying a previously developed generic 5 kW simple-cycle SOFC system. Fuel cell model modifications include changes in methods and constants for estimating over-potentials to better simulate a modern anode-supported planar SOFC. In addition to scaling up and modifying the fuel cell model, a thermal energy storage (TES) tank, exhaust gas duct burner and hot water exhaust gas recuperator model were integrated into the system model. The fully integrated system model can effectively simulate an SOFC-CHP system and evaluate the system performance and efficiency in meeting building electricity and heating demand profiles. For the present effort, dynamic building electricity and heating data from a hotel operated in Orange County, southern California during the months of July and August 2008 were analyzed.

Specifically, tradeoffs between SOFC performance and thermal energy storage have been investigated. The simulation results show that the SOFC-CHP system has the ability to follow the dynamic electrical load with appropriate system design and controls. Due to thermal power mismatch during electricity load-following operation, supplementary exhaust gas duct burner heat and/or a TES is required to independently dispatch the fuel cell power and meet the hotel heating demand. However, if the fuel cell is sufficiently sized, the system can achieve greater than 70% efficiency with only a small TES tank and without the need to fire the duct burner. The dynamic model and integrated SOFC-TES concept are shown to be useful for developing integrated CHP systems and to evaluate performance.

Keywords: Dynamic modeling, CHP, SOFC, thermal energy storage (TES)

1. INTRODUCTION

Combined Heat and Power (CHP) systems based on integrated solid oxide fuel cells (SOFC) are considered to be attractive future energy systems [1-6]. SOFC systems generate electricity with high thermal efficiency and low emissions and can also generate high quality heat. Very high overall efficiencies (>80%) can be achieved in natural gas and biogas fueled combined heat and power applications [1]. One major challenge for achieving such efficiencies is presented by the non-coincident and dynamic thermal and electrical demand profiles of many applications.

In addition to meeting local dynamic thermal and electrical demands, SOFC-CHP systems that can load-follow may be used to support the utility grid with increased renewable energy use. Grid dynamics will become more critically important to manage with increased intermittent and dynamic renewable power use. Therefore, SOFC-CHP systems that can provide dispatchable generation for the grid and/or directly handle local electrical load dynamics can provide a very beneficial resource for grid stability. Use of SOFC-CHP systems for this purpose will require the independent dispatch of heat for thermal integration and electricity for grid support. Thermal energy storage (TES) can provide the opportunity for the generator to follow electric loads while independently dispatching heat by receiving and releasing the generator heat according to local heat demands. The independent dispatch of CHP heat and

NOMENCLATURE

A	Surface Area [m^2]
C	Solid specific heat capacity [kJ kg^{-1} K^{-1}], Molar concentration of control volume [kmol m^{-3}]
C_V	Ideal gas constant volume specific heat capacity [kJ kmol^{-1} K^{-1}]
C_p	Ideal gas constant pressure specific heat capacity [kJ kmol^{-1} K^{-1}]
D_{H}	Hydraulic diameter [m]
D_{TES}	TES tank diameter [m]
E_{Nernst}	Nernst potential [V]
F	Faraday's constant [96,487 C mol^{-1}]
ΔG_{f}	Change in Gibbs free energy of formation [kJ kmol^{-1}]
H_{TES}	TES tank height [m]
h	Enthalpy [kJ kmol^{-1}], Convective heat transfer coefficient [kW m^{-2} K^{-1}]
h_{f}	Enthalpy of formation [kJ kmol^{-1}]
i	Electrical current [A]
j	Current density [A m^{-2}]
j_{o}	Exchange current density [A m^{-2}]
j_{L}	Limiting current density [A m^{-2}]
k	Conduction heat transfer coefficient [kW m^{-1} K^{-1}]
L	Length [m]
N	Control volume molar capacity [kmol]
$\dot{N}$	Molar flow rate [kmol s^{-1}]
n	Number of participating electrons in the reaction [-]
P	Power [kW]
P_i	Partial pressure of gas [atm]
q	Heat transfer [kW]
$\dot{Q}_{in}$	Heat transfer into control volume [kW]
R	Universal gas constant [8.3145 kJ kmol^{-1} K^{-1}],
T	Control volume temperature [K]
U_{fuel}	Fuel utilization [-]
V	Volume [m^3], Voltage [V]
V_{TES}	TES tank volume [Gallon]
V_{act}	Activation polarization [V]
V_{conc}	Concentration polarization [V]
V_{ohm}	Ohmic polarization [V]
$\dot{W}_{out}$	Work out of control volume [kW]
X	Species molar concentration [-]

electricity will allow thermally integrated distributed generators to better support the renewable energy based utility grid of the future.

However, control strategies for following the heat demand, as well as supporting the utility grid have not yet been developed. Therefore, studies of the detailed dynamic performance of these types of systems are required to enable design and control systems development for dispatchable SOFC-CHP systems.

In the present work, a dynamic model for a SOFC-CHP system has been developed based on an existing SOFC model. The dynamic simulation of this system (shown in Figure 1) is used to advance fuel cell dynamic understanding and controls to improve system dynamics and operating flexibility. Based on the measured hotel electricity and heating data, three system operating scenarios are simulated. Through the simulations, the thermal integration strategy and performance of SOFC systems with TES are investigated and discussed.

2. SOFC-CHP SYSTEM MODEL DESCRIPTION

A dynamic SOFC-CHP system model has been developed in a Matlab/Simulink® environment, considering mass balance, energy balance, chemical and electrochemical reactions, electrochemical losses, and heat transfer. The dynamic model is based on scaling up and modifying a previously developed validated model of a generic 5 kW simple-cycle SOFC system. For details regarding the fuel cell system models please see [7-10]. The purpose of the current model is to investigate the operating limits and improve the dynamic operating flexibility of SOFC-CHP systems with thermal energy storage and to demonstrate an ability to independently dispatch the system electricity and heat.

A schematic of the SOFC-CHP system simulated is shown in Figure 1. Major modifications of the original SOFC system model were made and additional component models (e.g. TES, heat exchanger, and exhaust gas duct burner) were developed and simulated using a similar modeling methodology. Only the modifications and additional model developments are described in the following section.

Modification and scale up of the original SOFC model

The dynamic model for a generic 5 kW simple-cycle system captures key design features that are included for load following capability as presented by Mueller *et al.* [7].

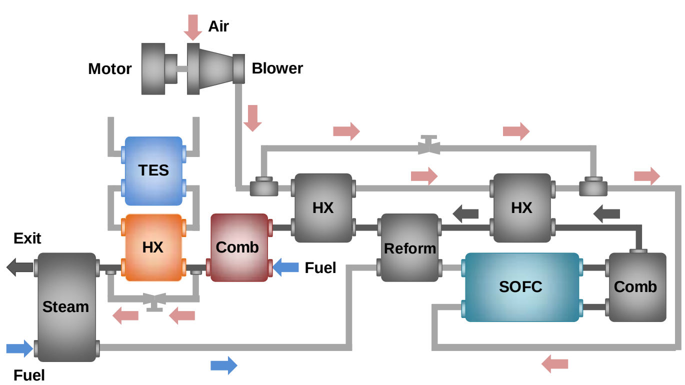

Fig.1 Schematic of the SOFC-CHP integrated system.

Modifications in the present work include changes in methods and constants for estimating over-potentials to better simulate a modern anode-supported planar SOFC. The fuel cell voltage in the model is calculated by subtracting activation, Ohmic, and concentration losses from the Nernst potential. The Nernst equation is solved accounting for local temperature and both anode and cathode partial pressures.

The Butler-Volmer equation with a transfer coefficient of 0.5 (Equation (1)) was used in place of a Tafel expression to calculate activation polarization. Furthermore, the performance of the model was found to be low compared to the present state-of-the-art planar SOFC. A sensitivity analysis was conducted in which the fixed parameters for calculating electrochemical losses were varied. This resulted in the selection of SOFC voltage model parameters as shown in Table 1.

$$V_{\text{act}} = \frac{2RT}{nF}\sinh^{-1}\left(\frac{j}{2j_L}\right) \tag{1}$$

After these modifications, the generic 5 kW simple-cycle system model was scaled up for the desired operating system power by increasing the number of fuel cell stacks, and balance of plant component sizes (e.g. heat exchanger plates, exhaust gas duct burner, and reformer).

Thermal energy storage (TES) tank

A dynamic TES model has been added to the integrated SOFC system model according to the schematic of Figure 1. The TES is modeled as presented in [11]. Several assumptions are made in the development of the equations solved in each of the TES control volumes:

(1) Mass flow occurs only in one direction either from top to bottom or bottom to top.
(2) Working fluid: liquid water.
(3) No heat transfer to the environment is allowed. The tank is assumed to be well insulated from the environment.
(4) Between control volumes, only mass transport and conductive heat transfer is considered.

Based on these assumptions, the molar flow rate and temperature of each control volume of the TES are determined from the appropriate transient energy and mass conservation equations of the same general form. Figure 2 shows the schematic of the modeled stratified thermal energy storage tank. The flow rates throughout the tank are calculated by the mass conservation equation in each control volume as follows.

Table 1 Important SOFC model parameters.

Number of cells	115	-
Area of a cell	0.01	m^2
Exchange current density	4,000	$A\,m^{-2}$
Limiting current density	9,000	$A\,m^{-2}$
Transfer coefficient	0.5	-
Resistance	$T\exp[7509.6/T\text{-}25.855]$	Ω

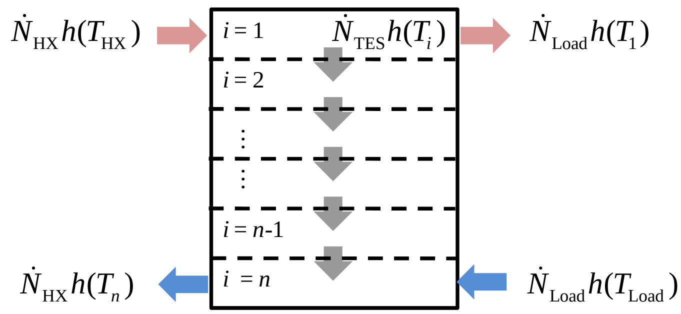

Fig. 2 Schematic of modeled thermal energy storage tank, showing model nodes and internal flow configuration.

$$\dot{N}_{\text{HX}} = \dot{N}_{\text{TES}} + \dot{N}_{\text{Load}} \tag{2}$$

where $\dot{N}_{\text{HX}}$, $\dot{N}_{\text{TES}}$, and $\dot{N}_{\text{Load}}$ show flow rate of the heat exchanger, internal flow rate of the TES tank, and flow rate of the hot water-exhaust gas recuperator respectively.

Temperature at each control volume is evaluated from transient energy conservation equation. Flow direction from top to bottom is assumed to be positive.

$$\dot{N}C_V\frac{dT}{dt} = \dot{N}_{\text{in}}h_{\text{in}} - \dot{N}_{\text{out}}h_{\text{out}} + \sum\dot{Q}_{\text{in}} - \sum\dot{W}_{\text{out}} \tag{3}$$

i) $i = 1$

$$\dot{N}_1C_V\frac{dT}{dt} = \dot{N}_{\text{HX}}h(T_{\text{HX}}) - \dot{N}_{\text{Load}}h(T_1) - \dot{N}_{\text{TES}}h(T_1) + Q_{\text{in}} \tag{4}$$

ii) $1 < i < n$

$$\dot{N}_iC_V\frac{dT}{dt} = \dot{N}_{\text{TES}}h(T_{i-1}) - \dot{N}_{\text{TES}}h(T_i) + Q_{\text{in}} \tag{5}$$

iii) $i = n$

$$\dot{N}_nC_V\frac{dT}{dt} = \dot{N}_{\text{TES}}h(T_{n-1}) - \dot{N}_{\text{Load}}h(T_{\text{Load}}) + \dot{N}_{\text{HX}}h(T_n) + Q_{\text{in}} \tag{6}$$

where i is the number of control volumes.

Conductive heat transfer between nodes is solved using Fourier's law throughout the model. The properties of water for conductive heat transfer are used.

$$Q_{\text{in}} = \frac{kA}{L}(T_{i-1} - T_i) \tag{7}$$

TES model comparison to experimental data

Important model parameters and simulation conditions are provided in Table 2. All values correspond to the published

Table 2 Simulation conditions for validation of the TES model.

Number of nodes, n	50	-
Tank volume, V_{TES}	16,000	Gallon
Tank diameter, D_{TES}	2.95	m
Tank height, H_{TES}	8.85	m
Cross sectional area of the Tank, A	6.83	m^2
Distance between control volumes, L	0.177	m
Height to diameter ratio of the tank, H/D	3	-
Density of the liquid water, ρ	999.7	kg m^{-2}
Heat conductivity of water, k	0.00058	kW $m^{-1}K^{-1}$
Inlet/Outlet flow	0.1	kmol s^{-1}
Inlet temperature	60	F
Initial temperature	42	F
Ambient temperature, T_{amb}	77	F

experimental data [12] except for the geometric data of the tank. Since the literature did not mention the geometry of the tank, a column tank with height to diameter ratio of 3 is assumed in the current model.

Time ordinary differential equations for each control volume are solved using the Simulink® stiff differential equation solver ODE 15s. Dynamic simulation of a full discharge cycle has been conducted and compared to available experimental data as shown in Figure 3 (b). Note that this simulation is conducted for a TES that provides cooling water in order to compare with published experimental data [12].

Figure 3 shows the comparison of current TES simulation result to the literature experimental result. The plot in the simulation result shows the temperature distribution in the tank at 15, 100, 200 300, 400, and 520 minutes after the start of discharging, respectively. In the experimental result, the lines (called thermoclines) show the temperature distribution at each time. The simulation result shows the dynamic change of the thermoclines in the tank at the same times showing that the current TES model results correspond well with the experimental data.

Heat exchanger

A model for a heat exchanger that uses SOFC exhaust gas to generate hot water for the TES has also been developed and introduced into the integrated system model. The heat exchanger model is based on a flat plate counter flow heat exchanger as presented in [7]. No heat loss to the environment is considered.

Exhaust gas duct burner

A model for a supplementary exhaust gas duct burner has also been added to the modeled system. The duct burner is modeled as a single control volume combustor as presented in [8]. The duct burner is assumed to operate adiabatically with complete fuel oxidation. Note that this duct burner heats up the SOFC exhaust gas which temperature is much higher than ambient temperature (approximately 490 K). Therefore, the thermal efficiency of the duct burner is assumed to be 100 % (all the fuel heating value is used to heat hot water).

This additional duct burner is only fired when the TES is depleted and the heat generated from SOFC is not sufficient to

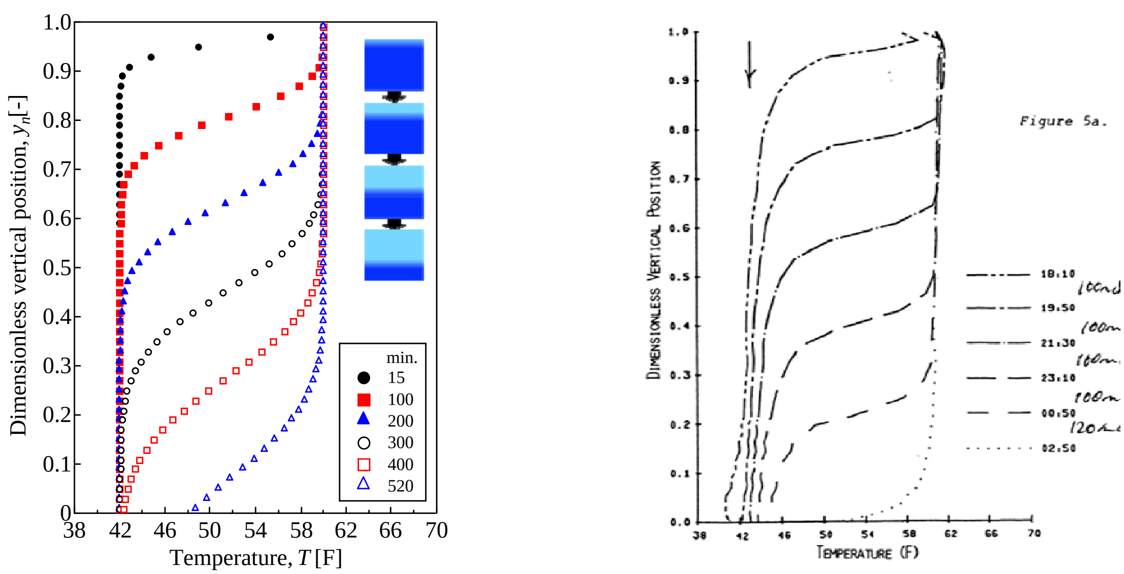

(a) Simulation result.

(b) Literature experimental data [12].

Fig. 3 Comparison of temperature distribution to experimental testing data, showing in full scale distributed nozzle tank during discharging for final cycle of complete charge-complete discharge test.

meet the instantaneous local heat demand. A control methodology for the duct burner is described in the following section.

System thermal integration and control methodology

In order to meet the local heat demand, heat generated by SOFC, heat from the duct burner and heat from the TES must be well controlled. When the SOFC generates the same amount of heat as the demand, heat from the duct burner and TES is not used. If the SOFC generates more heat than the demand, heat is stored in the TES until the tank becomes full. Once the tank is filled with hot water the hot water recuperator is bypassed and the exhaust gas from the SOFC goes directly into the fuel steam generator/fuel pre-heater. Meanwhile, if the heat generated from SOFC is not enough to meet the demand of the load, heat from the TES is dispatched. If the TES is depleted and the SOFC heat remains insufficient, the supplementary exhaust gas duct burner is operated to supply the required remaining heat. The size of the TES is designed to meet the amount of hot water demand for a day, which is approximately 50,000 gallons.

Two control loops have been added to the original fuel cell model for the system heat recovery components. The first control loop maintains the TES inlet temperature from the heat exchanger at a constant value by controlling the water flow rate of the heat exchanger (Figure 4). In this work, 360K which is 10 K above the temperature demand for the hotel hot water is applied (see the following measured data section). The second control loop maintains the TES outlet temperature above 350 K (the hotel's minimum hot water temperature requirement) by controlling the duct burner fuel flow rate (Figure 5). Note that the duct burner is only fired when the TES outlet temperature is below the demand temperature.

3. MEASURED DYNAMIC BUILDING ELECTRICAL AND THERMAL DATA

Dynamic building electricity and heating data were measured at a hotel operated in Orange County, southern California during the months of July and August 2008. Data

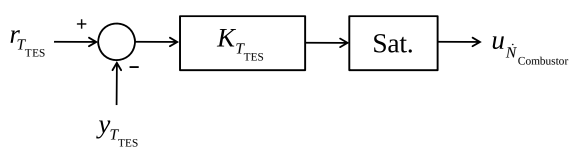

Fig. 4 Exhaust gas duct burner fuel flow rate controller.

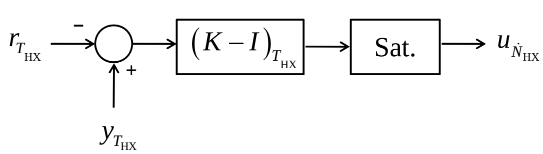

Fig. 5 Heat exchanger water flow rate controller.

were collected every 15 minutes. The main electric data for the facility is comprised of three separate meter readings. Total electrical energy demand is the sum of these three meter readings. The boiler load data includes flow rate and supply temperature of the water from the pipeline leading away from the main hotel boilers. A final hot water temperature of 160 F (344 K) is assumed since this temperature is closely controlled by the hotel boilers.

Figure 6 shows the electric and heating load demand for a week of July 30, 2008 to August 2, 2008. Compared to the electricity load, heat load more dramatically varies during a single day. In addition to the scattered distribution of the heating load, the maximum amount of heat power is approximately 1.5 times higher than the electricity demand. Considering these characteristics of the hotel demand, simple operation strategies for SOFC-CHP are suggested in the following section.

4. SYSTEM OPERATION STRATEGIES

Three basic operating strategies have been considered for the current SOFC-CHP system to meet local dynamic electricity and heating load demands. Basically, by controlling the SOFC output power, generated heat from the SOFC and exhaust gas duct burner is used to meet the hotel heating demand. As is described before, the amount of heating demand of the hotel is relatively large compared to the electric load. When the fuel cell power is equal to or less than the hotel heating load demand, heat must be produced by firing the duct burner to meet all of the heating demand. Three scenarios for operation are considered as the following:

Case 1: Base-load electricity operation, in which the SOFC electrical output is kept constant at approximately 10 % below the minimum electricity demand of the hotel.

Case 2: Electricity load-following operation, in which SOFC output follows the electricity demands of the hotel.

Case 3: High electricity base-load operation, in which SOFC output is maintained constant at the value that ends up producing sufficient heat from the SOFC to meet the maximum heat demand of the hotel with the TES.

Case 1 represents the typical current high temperature fuel cell system operating as a base-loaded system without exporting power to the grid as is required under Rule 21 – Generating Facility Requirement in California. In the future SOFC may be able to follow dynamic electric load profiles (case 2). Some recent research findings on SOFC control show that there is significant potential for SOFC to follow a variable and dynamic instantaneous load [8-10]. Finally case 3 is the scenario in which the SOFC-CHP system would be used as a decentralized power plant. The system meets the hotel heating demand as well as potentially exports extra electricity to support the utility grid network.

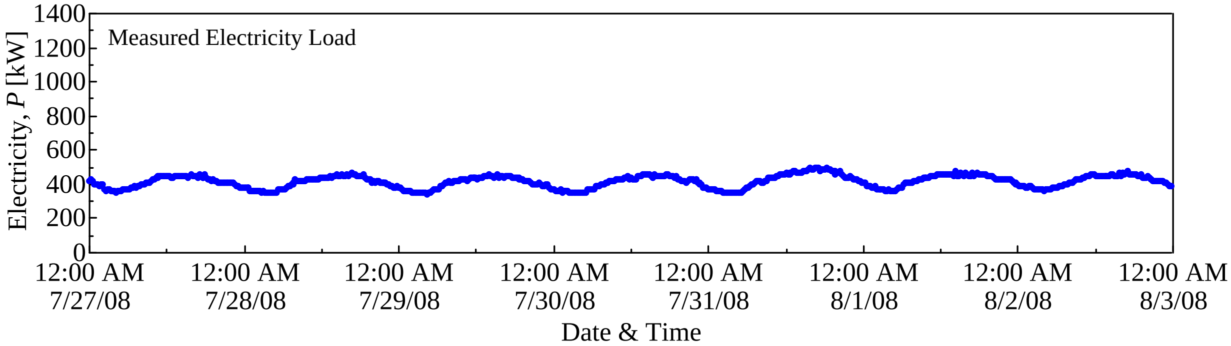

(a) Measured electricity demand.

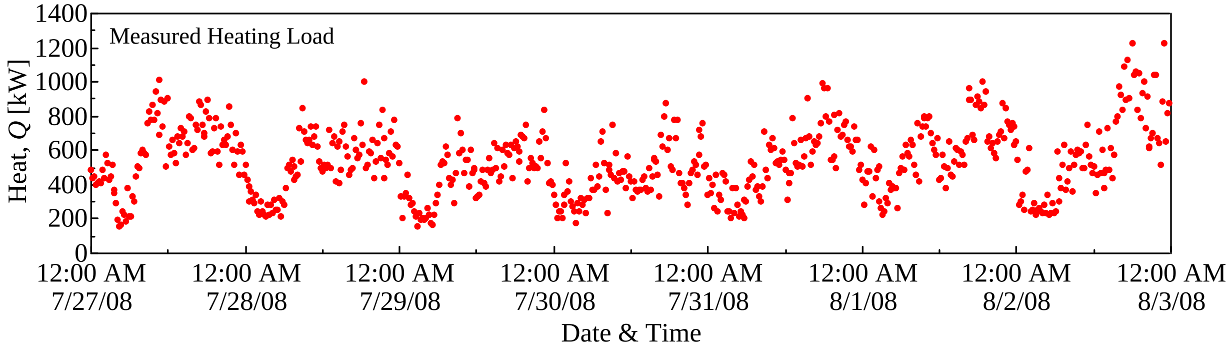

(b) Measured heating demand.

Fig. 6 The electric and heating load demand, which were obtained from a hotel operated in southern California from 12:00 a.m. on July 27, 2008 to 11:45 p.m. on August 2, 2008.

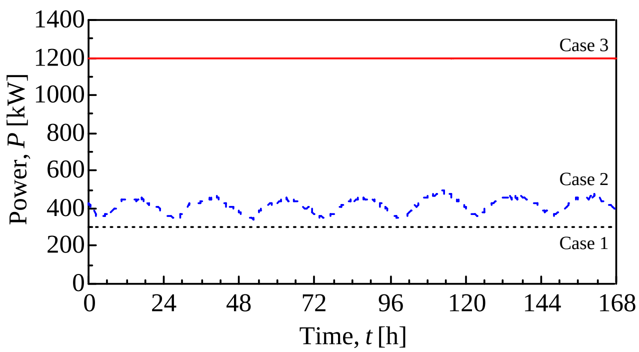

Fig. 7 Three operating scenarios for calculation.

Figure 7 shows three operating scenarios. For case 1 and case 3, operating voltage and fuel utilization are maintained at0.64V and 0.82, respectively. For case 2, operating voltage varies depending upon the electric load demand.

5. RESULTS AND DISCUSSION

These operating strategies are analyzed using the measured dynamic electricity and heating demand data as an input. This section includes three main sets of results that are important for SOFC-CHP system development: 1) dynamic heating demand and supply trends, 2) system performance in terms of thermal and electrochemical efficiency of the system, and 3) the effects of TES capacity and SOFC scale on the system performance.

Dynamic heat demand and supply

Figure 8 shows dynamic heating demand and supply using heat generated by SOFC, the exhaust gas duct burner, and the TES for all three cases. Recovered heat, $Q_{\text{recovered}}$, is defined as the amount of heat from the fuel cell transferred to heat up the hotel hot water supply. Note that a 3-day calculation result is shown in Figure 8 for each case. Heat from the additional duct burner and heat from SOFC are calculated by using the following equations, respectively.

$$\dot{Q}_{\text{recovered}} = \dot{N}_{\text{Load}} C_p \Delta T \tag{8}$$

$$\dot{Q}_{\text{comb}} = \dot{N}_{\text{add, fuel}} \text{LHV}_{\text{fuel}} \tag{9}$$

$$\dot{Q}_{\text{SOFC}} = \dot{N}_{\text{exhaust}} C_p \Delta T \tag{10}$$

In equation (8), ΔT is the difference between the temperature of cold water from the pipeline and the temperature of hot water supplied to the heat loop. Meanwhile, ΔT in equation (10) is the difference between the temperature of the SOFC exhaust gas and the system exit temperature, which is assumed to be 393 K.

Figure 8 shows that an appropriate amount of heat is supplied, for all the cases, by using SOFC generated heat and duct burner heat addition. For cases 1 and 2, the duct burner must be fired to meet the heat demand most of the time in a day (Figure 8 (a), (b)). Therefore, the TES tank never fills. In case 2, since SOFC power output corresponds to electricity demand

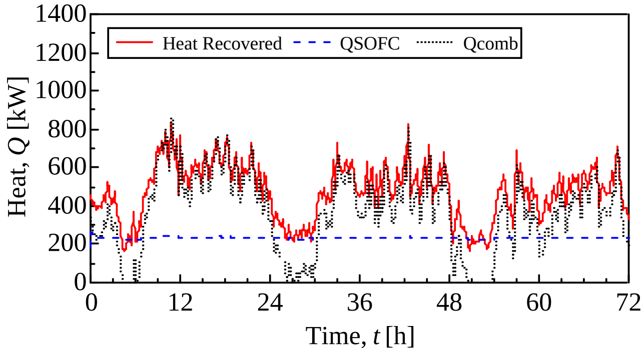

(a) Case 1.

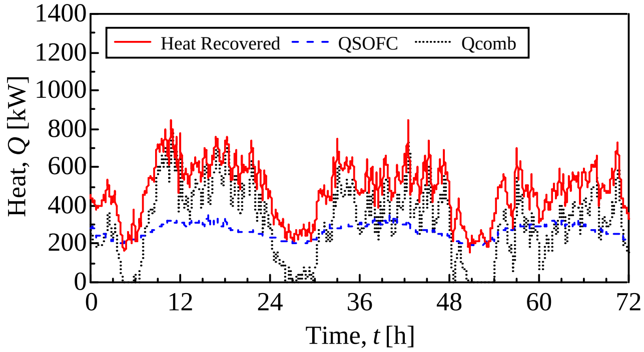

(b) Case 2.

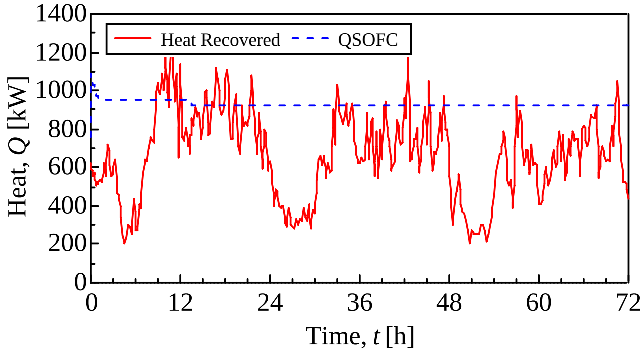

(c) Case 3.

Fig. 8 Dynamic heat demand and supply using generated heat by SOFC, additional combustor, and TES. (July 29-31, 2008)

(Figure 8 (b)), generated heat varies following the electricity load trend. For case 3, since the heat from the SOFC is enough to meet the heat demand, the duct burner no longer needs to be fired. In this case, the TES tank repeats a charge and discharge cycle depending upon the difference in generated heat and heating demand. Detailed profiles of the temperature distribution in the tank are described in a later section.

System performance

In this study, three efficiencies are defined as the following equations respectively:

$$\text{System Eff} = \frac{\text{Useful Energy}}{\text{Energy In}} = \frac{\dot{W}_{net} + \dot{Q}_{recovered}}{LHV_{SOFC} + LHV_{combustor}} \quad (11)$$

$$\text{SOFC Eff} = \frac{\text{SOFC Electricity}}{\text{SOFC Fuel}} = \frac{\dot{W}_{net}}{LHV_{SOFC}} \quad (12)$$

$$\text{SOFC-CHP Eff} = \frac{\text{SOFC Electricity and Heat}}{\text{SOFC Fuel}} = \frac{\dot{W}_{net} + \dot{Q}_{SOFC}}{LHV_{SOFC}} \quad (13)$$

where $\dot{W}_{net}$ is obtained by subtracting power of the blower from power output of the SOFC, $\dot{Q}_{recovered}$ and $\dot{Q}_{SOFC}$ are the same as previously defined in equations (9) and (11), respectively.

Figure 9 shows the comparison of these efficiencies for each case. In case 1 and case 3, both SOFC efficiency and SOFC-CHP efficiency remain constant because output electrical power is maintained at a constant value of 300 kW and 1200kW, respectively. On the other hand, in case 2, since the SOFC output power is controlled to follow the electricity demand of the hotel, SOFC efficiency, SOFC-CHP efficiency, and system efficiency vary with respect to time. The system efficiency of case 3 changes more dynamically because the SOFC-CHP system wastes some amount of the SOFC generated heat when the TES tank becomes full and bypasses the heat exchanger. However the results show that the system can achieve 70 % or greater average efficiency in all cases.

Temperature change in the TES

Figure 10 shows the dynamic temperature distribution change inside the TES tank for case 3. The initial condition of the TES tank is assumed to be full. As seen in Figure 10, when the heat generated from the SOFC exceeds the hotel heating demand, the TES starts charging. When heating demand increases, heat from the TES tank is dispatched to the hotel heating loop.

Although there is slight charging and discharging of the tank that occurs around midnight, overall the TES does not serve a useful purpose in both case 1 and case 2 because generated heat from the SOFC remains small compared to the heating demand.

TES capacity and SOFC power scale

Figure 11 shows the effects of TES capacity and SOFC power scale on SOFC-CHP performance and efficiency. As parameters, system efficiency and additional duct burner usage (defined in equation (14)), which are both calculated as an

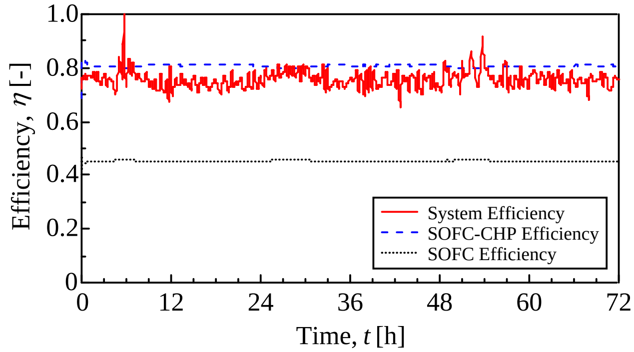

(a) Case 1.

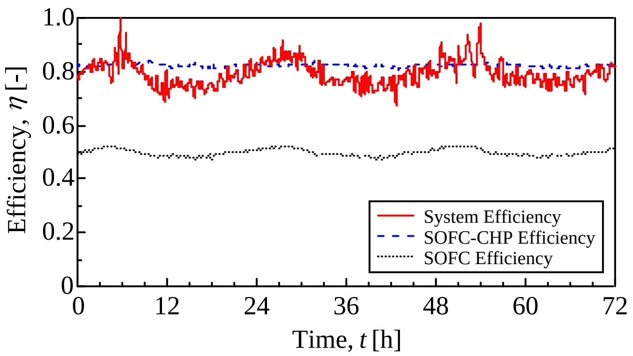

(b) Case 2.

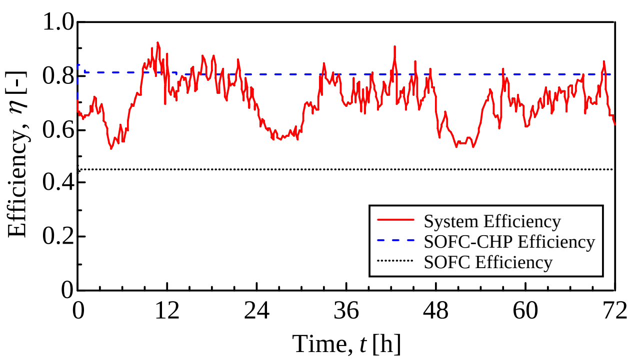

(c) Case 3.

Fig. 9 Comparison of SOFC efficiency, SOFC-CHP efficiency and system efficiency. (July 29-31, 2008)

average value for a week, are plotted as functions of SOFC output power for various TES capacity values. By and large, only a little difference in system efficiency and duct burner usage with regard to TES capacity is observed in the Figure 11. TES capacity has little or no effect on the calculated system efficiency.

$$\text{Duct burner Usage} = \frac{\int \dot{Q}_{\text{comb}} dt}{\int \dot{Q}_{\text{recovered}} dt} \qquad (14)$$

Three different ranges in SOFC scale however seem to be useful to understand the system performance. In Figure 11,

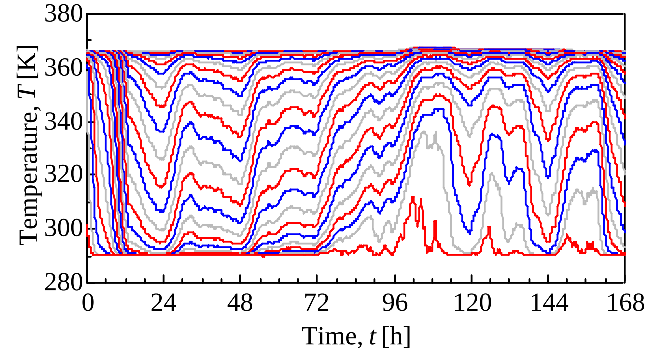

Fig. 10 Change in temperature distribution in TES during charge and discharge in case 3 (July 29, 2008 - August 2, 2008). Each line shows the temperature at the node in modeled TES tank.

system efficiency is extremely high in region I. Subsequently it remains constant in region II and then slightly decreases in region III as the SOFC becomes over-sized. The reason for high system efficiency in region I is that the duct burner efficiency in this model is nearly 100 %. Although current practical boiler efficiencies are approximately 80 %, the 100 % efficiency assumption is made because this duct burner heats up the SOFC exhaust gas as previously mentioned. The exhaust gas temperature is much higher than ambient temperature (approximately 490 K). This heat addition to the gas is assumed to be 100% followed by heat transfer to the water that occurs as it otherwise would from the SOFC exhaust gases alone. Therefore, all the heating value of the fuel is assumed to be used to heat hot water. The concept of this duct burner is shown in Figure 12. System efficiency in region II remains constant because the efficiency is determined by the trade off between duct burner usage and generated heat by the SOFC. The duct burner usage decreases as the heat from the SOFC increases. In region III, all the heat is supplied from the SOFC, i.e., the supplementary duct burner is never turned on. Therefore, the system efficiency goes down once the fuel cell is oversized and all the SOFC heat cannot be effectively utilized. For a given set of operating conditions based on the hotel data, the effects of the SOFC size on SOFC-CHP performance is more important than the effects of the tank capacity.

6. CONCLUSIONS

In order to understand and extend system operating limits and improve flexibility, a dynamic model of an SOFC-CHP system has been developed. The model is based upon a previously created and validated integrated SOFC system model. In addition to modification of electrochemical loss terms to simulate state-of-the-art planar SOFC performance, thermal energy storage (TES), exhaust gas duct burner, and heat exchanger models have been developed and integrated into the

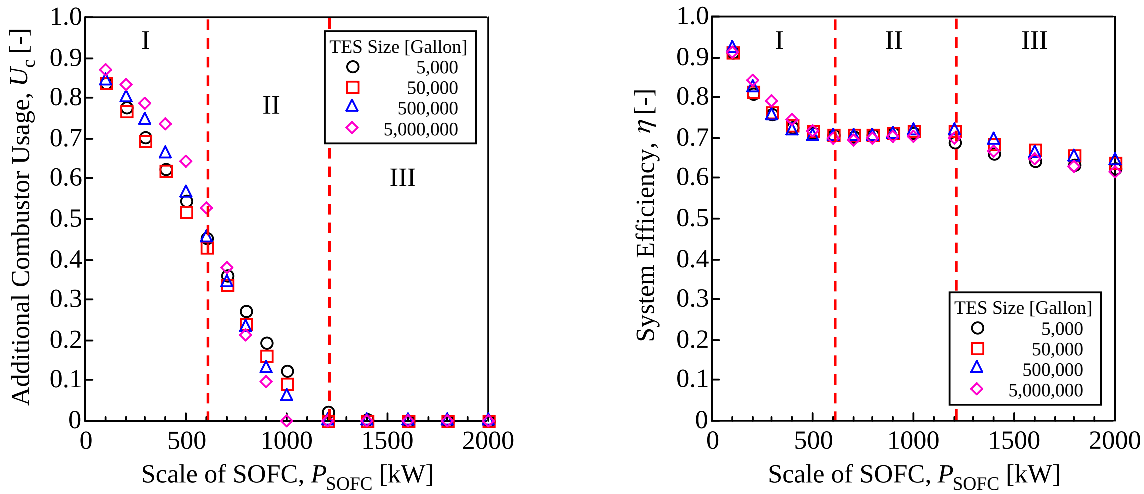

(a) Exhaust gas duct burner usage. (b) System efficiency.

Fig. 11 The effect of TES size and SOFC power scale on the CHP performance.

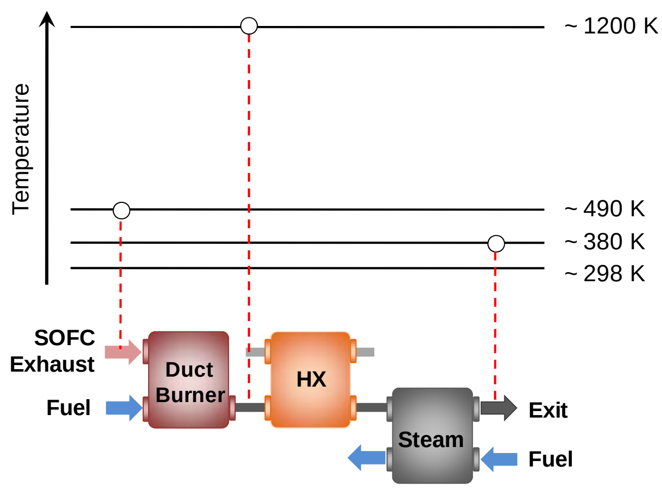

Fig. 12 Concept of an exhaust gas duct burner.

system to attempt to meet the local dynamic heat demand. The dynamic building electricity and heating data were obtained from a hotel operated in south Orange County in California during June and August of 2008.

Three basic strategies to operate SOFC-CHP system have been identified through the simulations using the developed dynamic model. The simulation results show an ability to follow the dynamic electrical load with appropriate system design and controls and to meet the local heating demand by scaling up of the exhaust gas duct burner and the TES. The results also demonstrate the impacts of the TES for supporting the SOFC performance in terms of the system thermal integration. The results further show the possibility for SOFC-CHP systems to export electricity to the grid to maximize overall system efficiency.

Even though the TES capacity and SOFC scale have little effect on the overall SOFC-CHP system performance, the TES adds operating flexibility. Furthermore, the SOFC-CHP system including TES could be used for not only hotels but also other building and built environment demands by appropriate thermal integration. Therefore, the dynamic model and integrated SOFC-TES concept itself are shown to be useful for developing integrated CHP systems to meet highly dynamic heating and electric load profiles.

ACKNOWLEDGMENT

This research has been carried out as part of a graduate exchange program between University of California and the University of Tokyo, Japan.

REFERENCES

[1] C-E Hubert, P. Achard, R. Metkemeijer, Study of a small heat and power PEM fuel cell system generator, Journal of Power Sources, **156**(2006), pp. 64-70

[2] I. Staffell, R. Green, K. Kendall, Cost targets for domestic fuel cell CHP, Journal of Power Sources, **181**(2008), pp. 339-349

[3] M. B. Blaeke, H. Lund, The effectiveness of storage and relocation options in renewable energy systems, Renewable Energy, **33**(2008), pp. 1499-1507

[4] D. W. Wu, R. Z. Wang, Combined cooling, heating, and power: A review, Progress in Energy and Combustion Science, **32**(2006), pp. 459-495

[5] G. Gigliucci, L. Petruzzi, E. Cerelli, A. Garzisi, A. La Mendola, Demonstration of a residential CHP system based on PEM fuel cells, Journal of Power Sources, **131**(2004), pp. 62-68

[6] P. A. Østergaard, Geographic aggregation and wind power output variance in Denmark, Energy, **33**(2008), pp.1453-1460

[7] F. Mueller, J. Brouwer, F. Jabbari, and S. Samuelsen, Dynamic simulation of an integrated solid oxide fuel cell system including current-based fuel flow control, Transactions of the ASME, **3**(2006), pp.144-154

[8] F. Mueller, R. Gaynor, A. E. Auld, J. Brouwer, F. Jabbari, G. S. Samuelsen, Synergetic integration of a gas turbine and solid oxide fuel cell for improved transient capability, Journal of Power Sources, **176**(2008), pp. 229-239

[9] K. Min, J. Brouwer, J. Auckland, F. Mueller, S. Samuelsen, Dynamic simulation of a stationary PEM fuel cell system, The 4th International Conference on Fuel Cell Science, Engineering and Technology, Irvine (2006), ASME

[10] F. Mueller, F. Jabbari, R. Gaynor, J. Brouwer, Novel solid oxide fuel cell system for rapid load following, Journal of Power Sources, **172**(2007), pp. 308-323

[11] S. Hermanns, Simulation of combined heating cooling and power equipment and application on two buildings powered by high temperature fuel cell-gas turbine hybrid systems, Thesis, Fachhochschule Trier Umwelt-Campus Birkenfeld, (2003), pp. 68-70

[12] M. W. Wildin and C. R. Truman, A summary of experience with stratified chilled water tanks, ASHRAE Transaction **20** Part1B (1985), pp. 956-976